Supporting Information

Ionic gel incorporating copper nanodots with antibacterial and antioxidant dual functions for deep tissue penetration treatment of periodontitis in rats

Yiru Gao, Wenxin Zhang, Rong Xue, Yang Shu*, Jianhua Wang*

Department of Chemistry, College of Sciences, Northeastern University, Shenyang, 110819, China

E-mail: shuyang@mail.neu.edu.cn (Y. Shu), jianhuajrz@mail.neu.edu.cn (J.H. Wang).

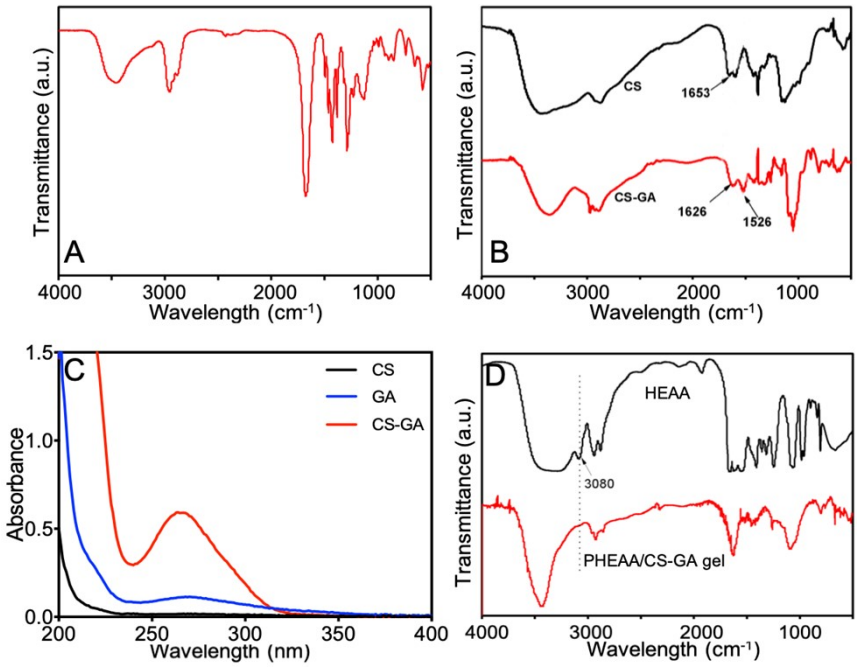

Figure S1. (A) FT-IR spectrum of Cu-NDs nanozymes. (B) FT-IR spectra of CS and CS-GA. (C) UV-vis absorption spectra of CS, GA and CS-GA. (D) FT-IR spectra of HEAA and PHEAA/CS-GA gel.

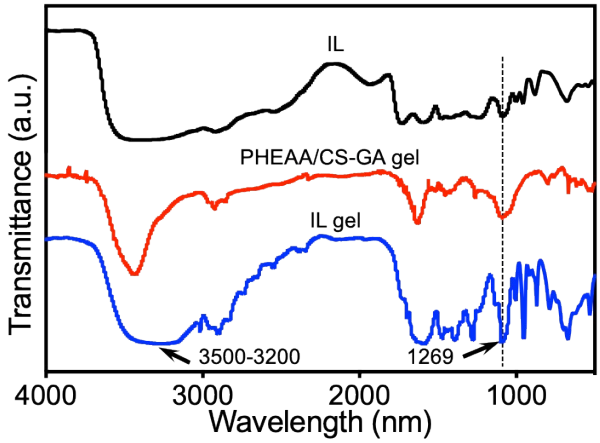

Figure S2. FT-IR spectra of IL, PHEAA/CS-GA gel and IL gel.

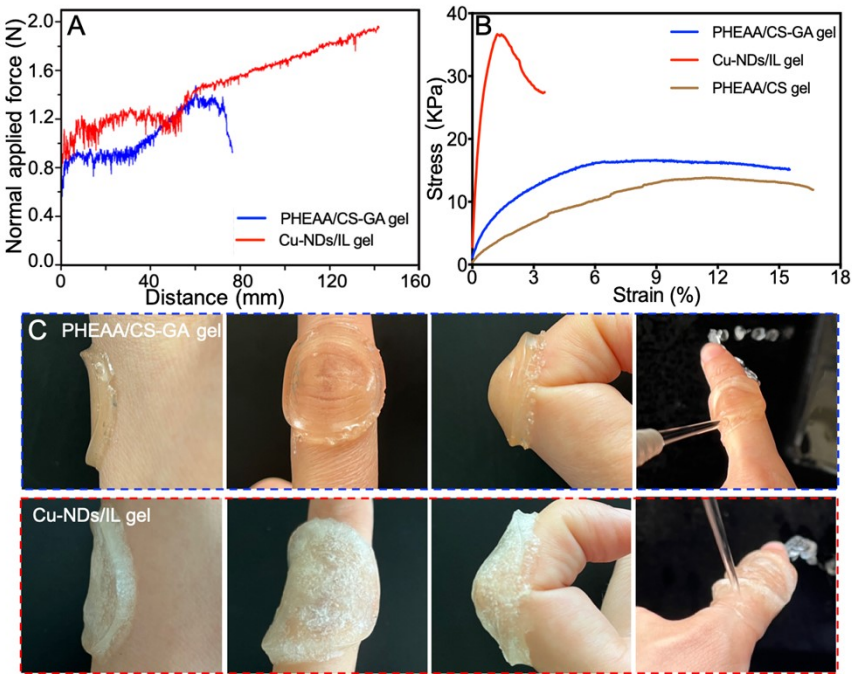

Figure S3. (A) Typical force–displacement curves for PHEAA/CS-GA gel and Cu-NDs /IL gel. (B) Lap-shear strength curves for PHEAA/CS gel, PHEAA/CS-GA gel and Cu-NDs /IL gel. (C) Photographs of PHEAA/CS-GA gel and Cu-NDs /IL gel adhered to skin. Photographs of PHEAA/CS-GA gel and Cu-NDs/IL gel adhered to different substrates.

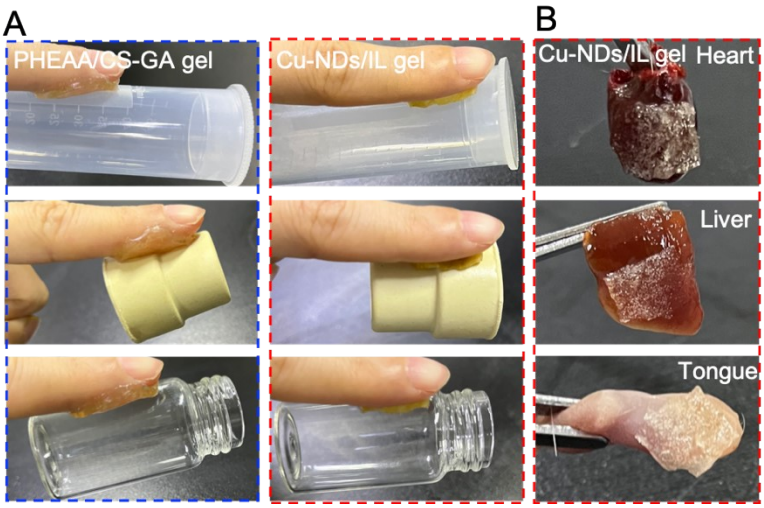

Figure S4. (A) Photographs of PHEAA/CS-GA gel and Cu-NDs/IL gel adhered to different substrates. (B) Photographs of PHEAA/CS-GA gel and Cu-NDs/IL gel adhered to moist biological tissues.

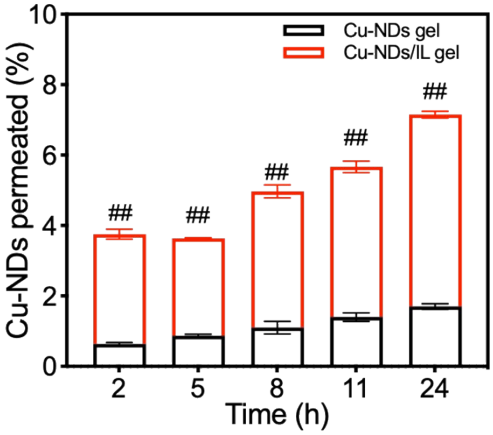

Figure S5. The cumulative percentage of Cu-NDs permeated after incubation with Cu-NDs gel and Cu-NDs/IL gel.

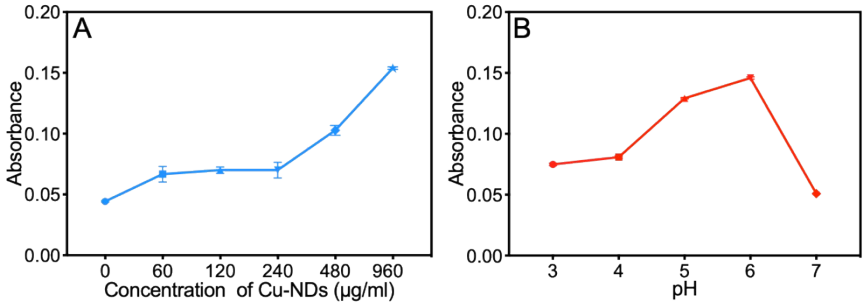

Figure S6. (A) The variations of POD-like activity at different concentrations of Cu-NDs (60, 120, 240, 480, and 960 μg/ml) with TMB (1 mM), H_2O_2 (2 mM) at pH 6. (B) The changes of POD-like activity of Cu-NDs at various pH values (pH 3, 4, 5, 6, and 7) with TMB (1 mM), Cu-NDs (960 μg/ml) and H_2O_2 (2 mM).

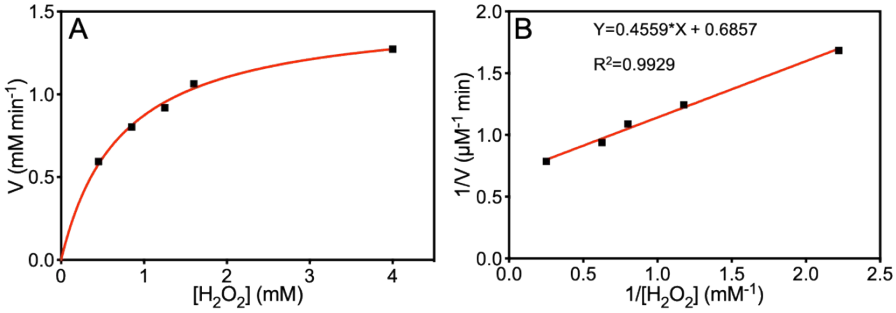

Figure S7. Michaelis-Menten kinetic analysis (A) and Lineweaver-Burk Fitting (B) of POD-like activity of Cu-NDs.

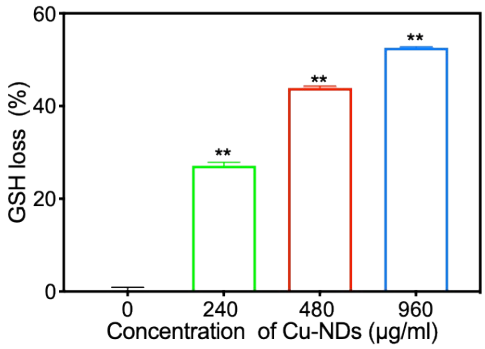

Figure S8. Percentage loss of GSH with the variation of Cu-NDs concentration (240, 480 and 960 μg/ml). GSH: 1 mM, DTNB: 0.1 mM.

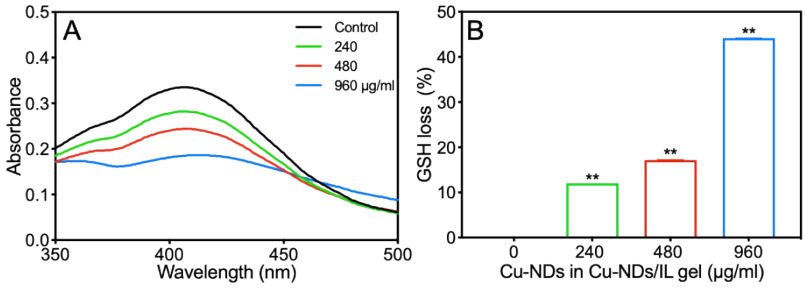

Figure S9. (A) GSH depletion in the presence of Cu-NDs/IL gel containing different concentrations of Cu-NDs (240, 480, and 960 μg/ml). (B) Percentage loss of GSH with Cu-NDs/IL gel containing different concentrations of Cu-NDs (240, 480, and 960 μg/ml), GSH: 1 mM, and DTNB: 0.1 mM.

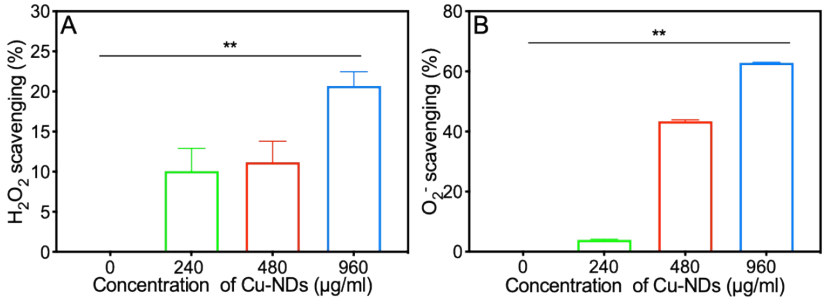

Figure S10. (A) H_2O_2 scavenging ratio of different concentration of Cu-NDs (0, 240, 480, and 960 μg/ml) with H_2O_2 (1 mM) at 37°C for 30 min. (B) $O_2^{\cdot -}$ scavenging ratios for different concentrations of Cu-NDs (240, 480, and 960 μg/ml) with riboflavin (20 μM), methionine (12.5 mM), NBT (75 μM) in PBS (pH 7.4) and irradiated with ultraviolet light for 20 min.

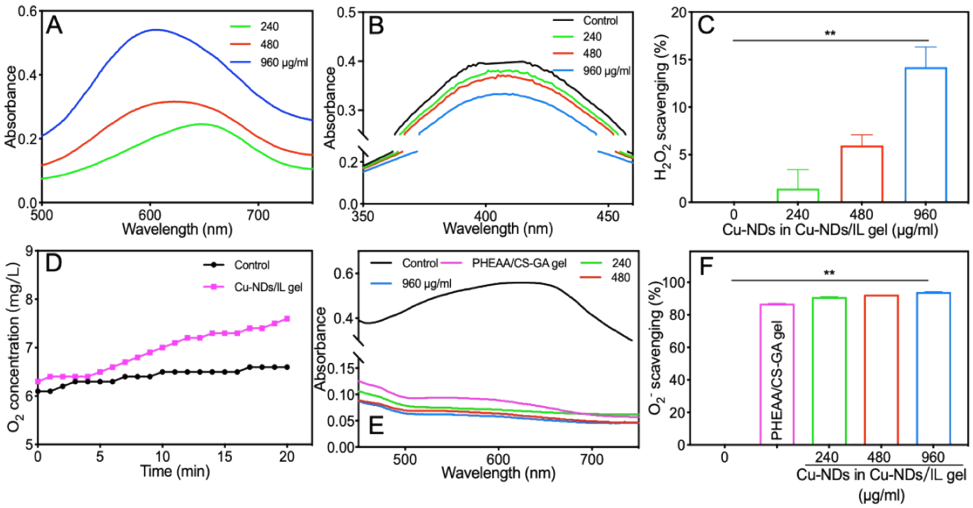

Figure S11. (A) UV-vis absorption spectra of TMB in the POD-like test of Cu-NDs/IL gel containing various concentrations of Cu-NDs (240, 480, and 960 μg/ml) with H_2O_2 (2 mM) and TMB (1 mM). (B) The variations of CAT-like activity of Cu-NDs/IL gel containing various concentrations of Cu-NDs (240, 480, and 960 μg/ml) with H_2O_2 (1 mM) at 37°C for 30 min. (C) H_2O_2 scavenging ratio of Cu-NDs/IL gel containing various concentrations of Cu-NDs (240, 480, and 960 μg/ml) with H_2O_2 (1 mM) at 37°C for 30 min. (D) Evaluation of CAT-like activity of Cu-NDs/IL gel through O_2 production at concentration of 240 μg/ml Cu-NDs in Cu-NDs/IL gel. (E) Assessment of SOD-like property of PHEAA/CS-GA gel and Cu-NDs/IL gel through $O_2^{\cdot-}$ elimination. (F) $O_2^{\cdot-}$ scavenging ratios of Cu-NDs/IL gel containing various concentrations of Cu-NDs (240, 480, and 960 μg/ml) and PHEAA/CS-GA gel (diameter 5 mm) with riboflavin (20 μM), methionine (12.5 mM), NBT (75 μM) in PBS (pH 7.4) and irradiated with ultraviolet light for 20 min.

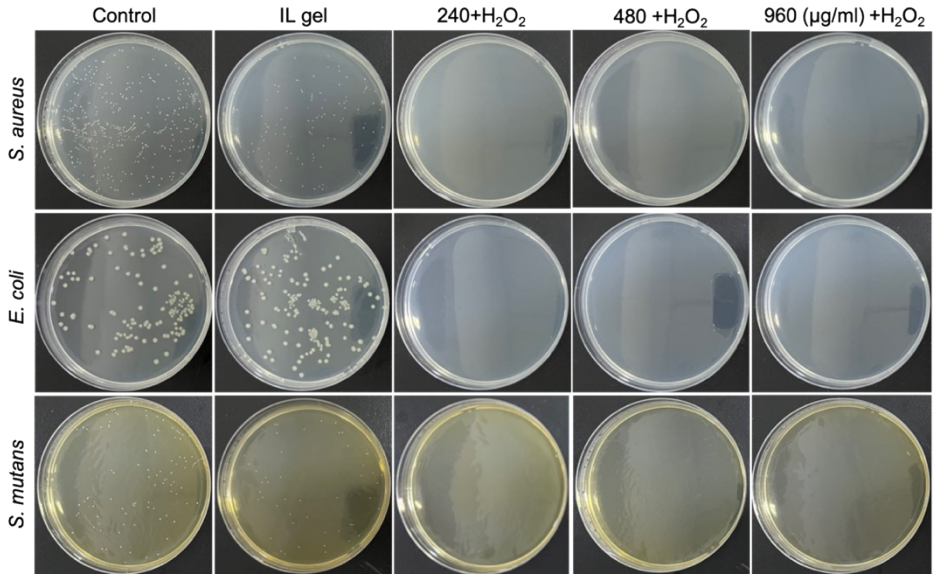

Figure S12. Representative photographs of bacteria cocultured with IL gel (5 mg/ml) or Cu-NDs/IL gel containing various concentrations of Cu-NDs (240, 480, and 960 μg/ml) with 500 μM H_2O_2.

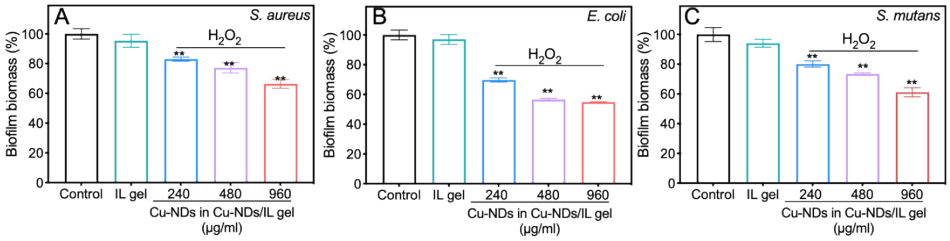

Figure S13. The antibiofilm effects of (A) *S. aureus*, (B) *E. coli* and (C) *S. mutanus* cocultured with IL gel (5 mg/ml) or Cu-NDs/IL gel containing various concentrations of Cu-NDs (240, 480, and 960 μg/ml) with 500 μM H_2O_2.

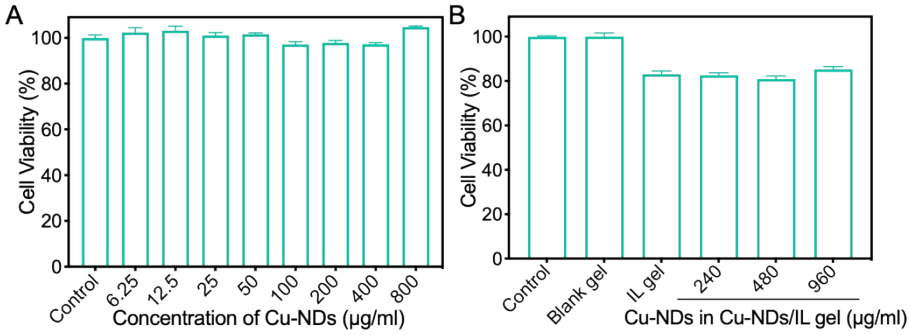

Figure S14. The viability of RAW 264.7 cells after incubation for 24 h with different concentrations of Cu-NDs (0-800 μg/ml) (A), blank gel, IL gel (IL: 5 mg/ml) or Cu-NDs/IL gel (containing 240, 480, and 960 μg/ml Cu-NDs) (B).

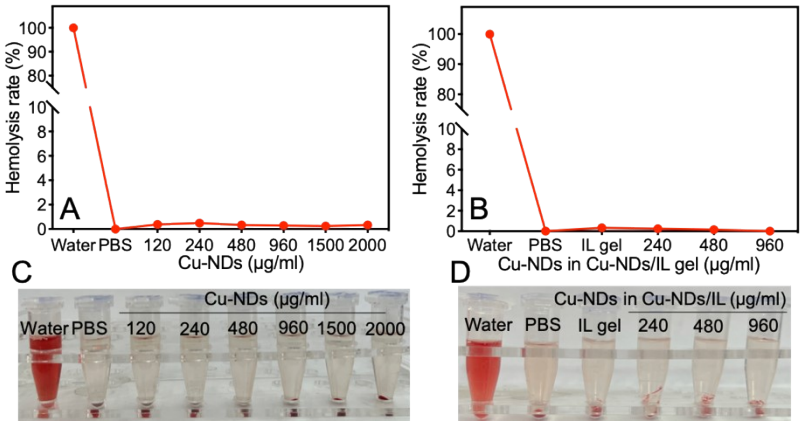

Figure S15. The hemolysis rate of blood cells by treatment with various concentrations of (A) Cu-NDs at 120, 240, 480, 960, 1500 and 2000 μg/ml, (B) IL gel (IL: 5 mg/ml) and Cu-NDs/IL gel (containing 240, 480, 960 μg/ml Cu-NDs). (C, D) The photographs of hemolysis in the above tests.

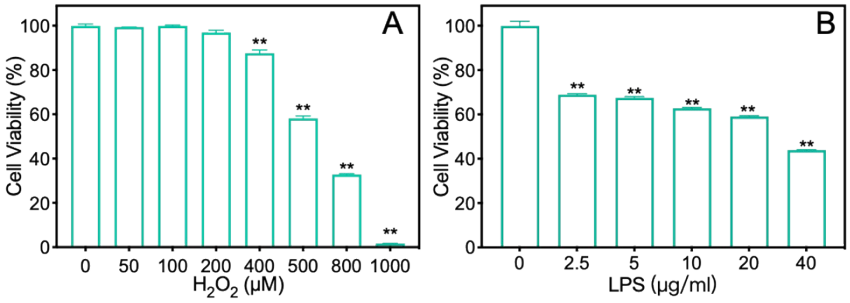

Figure S16. The viability of RAW 264.7 cells after incubation for 24 h with various concentrations of (A) H_2O_2 (50, 100, 200, 400, 500, 800, and 1000 μg/ml) and (B) LPS (2.5, 5, 10, 20, and 40 μg/ml) (B). ($n \geqq 3$, $^{**}p < 0.01$)

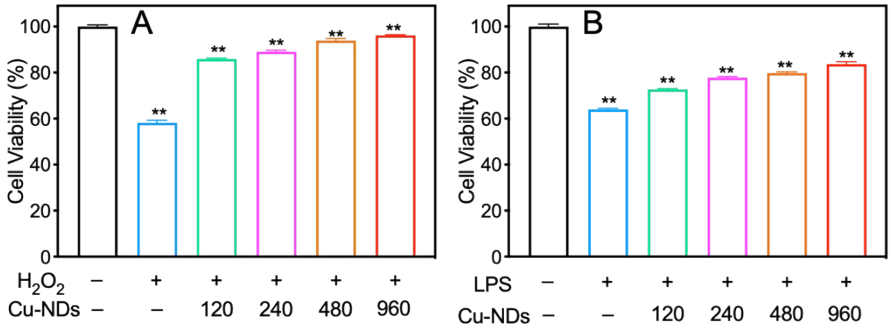

Figure S17. Cu-NDs (120, 240, 480, and 960 μg/ml) protecting RAW 264.7 cells from the oxidative stress caused by (A) H_2O_2 (500 μM) and (B) LPS (10 μg/ml) ($n \geqq 3$, $^{**}p < 0.01$).

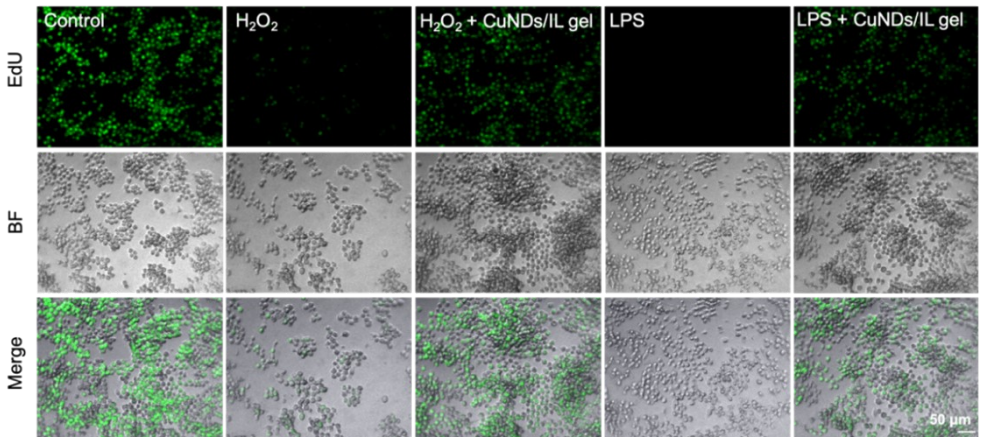

Figure S18. CLSM images of RAW 264.7 cells after different treatments with EdU staining to serve as proliferation indicator. H_2O_2: 500 μM, LPS: 10 μg/ml, Cu-NDs/IL gel: containing 480 μg/ml Cu-NDs. BF was bright field.

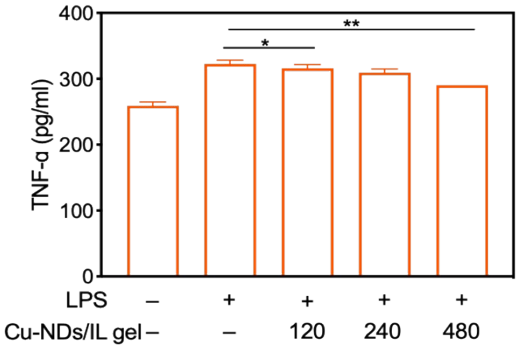

Figure S19. The expression of TNF-α after LPS (10 μg/ml) and Cu-NDs/IL gel treatment (containing 120, 480, and 960 μg/ml Cu-NDs). ($n \geqq 3$, * $p < 0.05$, ** $p < 0.01$).

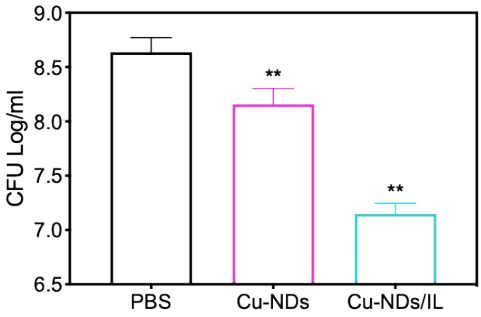

Figure S20. CFU numbers of gingival tissues after treatment with 960 μg/ml Cu-NDs gel and Cu-NDs/IL gel (containing 960 μg/ml Cu-NDs).

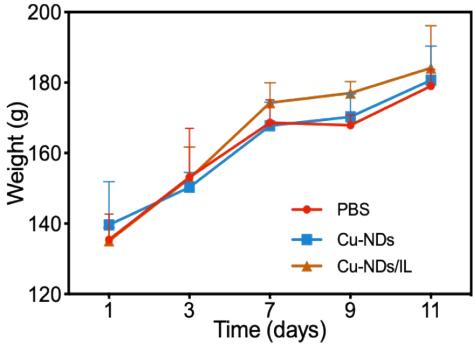

Figure S21. Body weight changes of the rats during the period of various treatments.

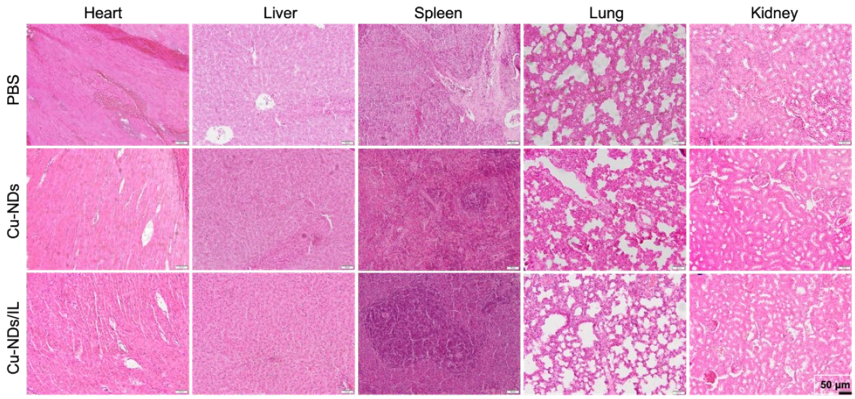

Figure S22. H&E staining of heart, liver, spleen, lung and kidney after different treatments.

Catalyst	Substrate	K_m [mM]	V_{max} [μM min^{-1}]	Ref.
Cu-CD	H_2O_2	1.6	1.77 mgL^{-1} s^{-1}	1
SAFe-NMCNs	H_2O_2	0.63	0.756	2
C-NP	H_2O_2	0.38	0.246	3
C-NFs	H_2O_2	0.31	2.480	3
HMSN@Au	H_2O_2	50.76	23.712	4
Cu-NDs	H_2O_2	0.66	1.458	This work

Table S1. Steady-state kinetic parameters of various nanozymes and Cu-NDs with H_2O_2 as the substrate for POD-like catalysis.

References

1 M. Liu, L. Huang, X. Xu, X. Wei, X. Yang, X. Li, B. Wang, Y. Xu, L. Li and Z. Yang, *ACS Nano*, 2022, **16**, 9479–9497.

2 Y. Su, F. Wu, Q. Song, M. Wu, M. Mohammadniaei, T. Zhang, B. Liu, S. Wu, M. Zhang, A. Li and J. Shen, *Biomaterials*, 2022, **281**, 121325.

3 Y. Xing, L. Wang, L. Wang, J. Huang, S. Wang, X. Xie, J. Zhu, T. Ding, K. Cai and J. Zhang, *Adv. Funct. Mater.*, 2022, **32**, 2111171.

4 M. Chen, J. Song, J. Zhu, G. Hong, J. An, E. Feng, X. Peng and F. Song, *Adv. Healthc. Mater.*, 2021, **10**, 2101049.